# Morphological Appearance Manifolds in Computational Anatomy: Groupwise Registration and Morphological Analysis

Nai-Xiang Lian*, and Christos Davatzikos

Department of Radiology,
University of Pennsylvania, Philadelphia, PA

**Abstract.** The field of computational anatomy has developed rigorous frameworks for analyzing anatomical shape, based on diffeomorphic transformations of a template. However, differences in algorithms used for template warping, in regularization parameters, and in the template itself, lead to different representations of the same anatomy. Variations of these parameters are considered as confounding factors. Recently, extensions of the conventional computational anatomy framework to account for such confounding variations has shown that learning the equivalence class derived from the multitude of representations can lead to improved and more stable morphological descriptors. Herein, we follow that approach, estimating the morphological appearance manifold obtained by varying parameters of the template warping procedure. Our approach parallels work in the computer vision field, in which variations lighting, pose and other parameters leads to image appearance manifolds representing the exact same figure in different ways.
The proposed framework is then used for groupwise registration and statistical analysis of biomedical images, by employing a minimum variance criterion to perform manifold-constrained optimization, i.e. to traverse each individual's morphological appearance manifold until all individuals' representations come as close to each other as possible. Effectively, this process removes the aforementioned confounding effects and potentially leads to morphological representations reflecting purely biological variations, instead of variations introduced by modeling assumptions and parameter settings. The nonlinearity of a morphological appearance manifold is treated via local approximations of the manifold via PCA.

## 1 Introduction

Computational anatomy provides a powerful tool for characterizing differences between normal and pathologic anatomies by analyzing their variations relative to a common template. Diffeomorphic shape transformations [1–3] are first estimated to warp all anatomies to a template or vice versa; various descriptors are then derived to quantify their morphological characteristics.

Template transformations are often derived from image similarity measures, in the intensity-driven methods [1, 4], either by employing intensity differences

* This work was supported by the NIH-funded Grant R01-CA104976.

or via mutual information [3, 5]. Topology is maintained by imposing smoothness constraints either via physical models [1, 6] or directly on the deformation field [7]. Other approaches, such as [3, 5], ensure biological correspondence through feature-based approaches by introducing biologically, anatomically and geometrically significant attributes in shape morphological representations.

Various approaches have been presented in the literature, under the umbrella of computational anatomy: *large deformation diffeomorphic metric mapping* (LDDMM) [8], *deformation based morphometry* (DBM) [9, 10], *voxel based morphometry* (VBM) [11, 12], *tensor based morphometry* (TBM) [13], depending on the aspects of the template transformation being measured. DBM, for instance, establishes group differences based on local deformation of anatomical structures through the Jacobian of the diffeomorphism. VBM, on the other hand, factors out global differences via diffeomorphism, before analyzing anatomical differences. VBM is, therefore, considered as complementary to DBM, since the former utilizes the information not represented by the transformation.

However, the inherent complexity of the problem poses a major challenge to these approaches. First, anatomical correspondence may not be uniquely determined from intensity-based image attributes, which drive template warping algorithms. Second, exact anatomical correspondence may not exist at all due to anatomical variability across subjects. As a result, the choice of the template plays an important role in the accuracy of analysis. The aforementioned challenges lead to residual information that the transformation fails to capture.

To remedy this problem, some approaches have been proposed to use average anatomies as templates [14], to facilitate the template matching procedure. In most practical cases, considerable differences still persist between samples and the average brain. A very promising approach in this situation is groupwise registration [15, 16], which solves the problem to a certain extent, in the sense that instead of minimizing individual dissimilarity it minimizes combined cost. Bhatia et al. [15], for instance, implicitly find the common coordinate system by constraining the sum of all deformations from itself to each subject to be zero. Davis et al. [14] compute the most representative template image through a combined cost functional on the diffeomorphism group of spatial deformations. Such groupwise registration based representations are, therefore, more consistent across the samples, even though they might still fail to eliminate residuals.

In the approach presented herein, we follow the work of [17], which uses a complete morphological descriptor of the form [Transformation, Residual]; any morphological information not captured by the transformation is captured by the residual, hence no morphological characteristic is discarded. An entire class of many anatomically equivalent descriptors is generated by varying parameters of the template transformation, as well as the template itself, all representing the same anatomy. The resultant anatomical equivalence class (AEC) maps the underlying anatomy to a manifold embedded in a high dimensional space, which we call a *morphological appearance manifold* (MAM). Although such manifolds can be nowhere differentiable [18], they can become differentiable by smoothing the images. Instead of directly smoothing the images prior to estimating a

MAM, we estimate its local structure by fitting a hyperplane that approximates its tangent plane, as described below. In a group-wise registration framework, among the members of an AEC of each individual, one is selected according to the criterion that the variance across individuals is minimized. This problem is solved via a manifold-constrained optimization approach, which locally estimates the structure of the MAM via local PCA, and moves along the manifold to minimize the variance across individuals. Intermediate steps of projection onto the manifold are necessary to guarantee that each individual's representation remains on its respective manifold. Standard voxel-based analysis methods are then used to compare individuals and groups, however they are applied to the optimal morphological signatures (OMS) obtained through this optimization. Unlike the work in [17], which used a globally linear approximation, by using a local approximation of the MAM we follow the nonlinearities of the underlying AEC.

In practice, it is impossible to sample all possible diffeomorphisms and respective residuals. Therefore, we have chosen to vary the two most important sources of variation in practice: the regularization strength, which determines how aggressive the template warping is; and the template, whose similarity with an individual anatomy can significantly affect the resultant morphological representation. By varying these two factors, we obtain an estimate of the structure of the MAM of each individual. An optimization approach then allows the representation of each individual anatomy to traverse its respective MAM, until a minimum variance criterion in the entire group is achieved.

The approach described herein is akin to methods on image appearance manifolds that have been used in computer vision [19] to model variations in images that are caused by measurement parameters, such as illumination and pose. Such variations are confounding factors when, for example, one is interested in face recognition, as the same person appears different for different parameters. As in our work, learning such variations is important for determining robust parameters to be used for analysis and recognition.

## 2 Morphological Appearance Manifold of an Anatomical Equivalence Class

Computational anatomy involves characterizing anatomical differences between a subject $S$ and a template $T$ by mapping the template space $\Omega_T$ to the subject space $\Omega_S$ through a diffeomorphism $h : \Omega_T \rightarrow \Omega_S, \mathbf{x} \mapsto h(\mathbf{x})$ by maximizing some similarity criterion between $T$ and normalized subject $S_T$. A zero residual mapping is usually not possible or even not-existent, resulting in a residual:

$$R_h(\mathbf{x}) := T(\mathbf{x}) - S(h(\mathbf{x})), \mathbf{x} \in \Omega_T \tag{1}$$

Our approach herein is to use a template warping algorithm that captures some of the morphological differences between the template and the target anatomies, in combination with the respective residual, which captures everything else. In [17], the transformation and the residual were combined into a concatenated

descriptor: $(h, R_h)$. In our work, we adopt a slightly different way of combining $h(.)$ and $R_h(.)$, for two reasons. First, it is not intuitive how the transformation and the residual should be weighted, relative to each other, when calculating distances. Second, in applying this approach to medical image analysis problems, we are primarily interested in quantifying patterns of local variations of sizes of biological tissues, as, for example, brain atrophy. Such local volumetric measurements can be quantified by RAVENS maps [12], defined as follows:

$$\mathcal{Q}_h(\mathbf{x}) := J_h(\mathbf{x})[T(\mathbf{x}) - R_h(\mathbf{x})], \mathbf{x} \in \Omega_T, \tag{2}$$

where $J_h$ is the Jacobian determinant of the transformation $h$. For brevity, we refer to the morphological representation obtained via $\mathcal{Q}_h(.)$ as a complete morphological descriptor (CMD); the term "complete" stems from the fact that the residual completes the representation obtained via the transformation $h(.)$ so that no morphological information is discarded.

$\mathcal{Q}_h$, depends not only on the underlying anatomy but also on transformation parameters. An entire family of anatomically equivalent CMDs - they are equivalent to reconstruct the same anatomy, and form an (anatomical) equivalence class (AEC) - may be generated by varying $h$. In practice, it is impossible to sample all possible transformations and residuals to characterize an AEC, therefore we concentrate on two important parameters for variations of $h$: $h_{\lambda,\tau}$, where $\lambda$ denotes the amount of regularization and $\tau$ denotes an intermediate template. Since analysis eventually has to be carried out in a common space, we ultimately bring all anatomies to the template space $\Omega_T$, however intermediate templates capture the variation we expect to see when the same anatomy is seen "via different templates". Variations of the regularization parameter $\lambda$ reflect variations observed by varying the degree of conformality of the transformation, with large values of $\lambda$ indicating very smooth transformations and then large residuals, and $\lambda = 0$ indicating the most conforming transformation of the template under the assumptions of a respective deformable registration algorithm. For tractability and notational simplicity, we combine confounding factors together to represent $\boldsymbol{\theta} := (\tau, \lambda)$, and the corresponding definition of AEC becomes

$$\mathcal{A}(S) = \{\{(\mathcal{Q}_{h_{\boldsymbol{\theta}}}(\mathbf{x}) = J_{h_{\boldsymbol{\theta}}}(\mathbf{x}) S(h_{\boldsymbol{\theta}}(\mathbf{x}))) : S(h_{\boldsymbol{\theta}}(\mathbf{x})) = T(\mathbf{x}) - R_{h_{\boldsymbol{\theta}}}(\mathbf{x}), \quad \forall \mathbf{x} \in \Omega_T\}, \forall \boldsymbol{\theta} \in \boldsymbol{\Theta}\}$$

In the following section, we develop an optimization to determine the OMS from the MAM corresponding to an AEC, i.e. the optimal member of each individual's AEC, according to some criteria.

## 3 Finding the optimal point on the morphological appearance manifold

In order to derive a single representation out of an entire AEC, we will solve an optimization problem. First considering the simplest case of two subjects, we notice that if evaluating the similarity of two anatomies, we could find the minimum distance between the respective MAMs. Extending this idea to an arbitrary number of anatomies, we apply an optimization that allows sliding along

each individual MAM to find representations with minimum sum of squared distances of the entire group being registered. These representations best highlight differences between these anatomies, since together they eliminate confounding effects of $\lambda$ and $\tau$. For $L$ anatomies, we minimize sum of their squared distances, which is equivalent to optimizes the variance of morphological descriptors over entire ensemble w.r.t. confounding factors:

$$\boldsymbol{\Theta}^* = \arg \min_{\substack{\boldsymbol{\Theta}=(\boldsymbol{\theta}_1,\ldots,\boldsymbol{\theta}_L) \\ \mathcal{Q}_k(\boldsymbol{\theta}_k)\in\mathcal{A}(S_k),k=1,\ldots,L}} \sum_{i=1}^{L} d^2\left(\mathcal{Q}_i(\boldsymbol{\theta}_i), \bar{\mathcal{Q}}(\boldsymbol{\Theta})\right), \tag{3}$$

where $\mathcal{Q}_i(\boldsymbol{\theta}_i)$ is the CMD of subject $i$ for $\boldsymbol{\Theta} = (\boldsymbol{\theta}_1, \ldots, \boldsymbol{\theta}_L)$, and $\bar{\mathcal{Q}}(\boldsymbol{\Theta}) = \frac{1}{L}\sum_{i=1}^{L} \mathcal{Q}_i(\boldsymbol{\theta}_i)$ is the mean descriptor. $\boldsymbol{\Theta}^*$ represents the optimal selection of parameters, whose values differ for different individuals.

To optimize the criterion (3), we need to estimate the AEC. Practical considerations limit us to sampling the AEC at a discrete number of locations. Although a AEC resembles a generally nonlinear manifold, we assume linearity in a local neighborhood. The same assumption is used for the popular nonlinear approximation methods ISOMAP [20] and LLE [21]. Under this assumption, we apply principle component analysis (PCA) to represent the local neighborhood of the AEC manifold:

$$\mathcal{Q}_i^{(\delta\boldsymbol{\theta}_i^{center})}(\boldsymbol{\theta}_i) = \hat{\mathcal{Q}}_i^{(\delta\boldsymbol{\theta}_i^{center})} + \sum_{j=1}^{n} \alpha_{ij} V_{ij}^{(\delta\boldsymbol{\theta}_i^{center})} \tag{4}$$

where $\delta\boldsymbol{\theta}_i^{center}$ is the local neighborhood space around the center sample $\mathcal{Q}_i(\boldsymbol{\theta}_i^{center})$. This optimization problem is solved iteratively. During each iteration, the local linear approximation of the MAM is recomputed, centered on the current point on the manifold: $\boldsymbol{\theta}_i^{center} = \boldsymbol{\theta}_i^*$. We refer to this optimization process as manifold-constrained optimization (see Figure 1).

However, setting the current point as center for local MAM approximation could make the optimization vulnerable to local minima (see Figure 1). Increasing the neighborhood size used may solve the problem, but also lead to poor global linear approximation of a highly nonlinear manifold. To help avoid local minima without increasing neighborhood size, we set the center sample of each individual anatomy as the one nearest to the current mean descriptor, $\bar{\mathcal{Q}}(\boldsymbol{\Theta}^*) = \frac{1}{L}\sum_{i=1}^{L} \mathcal{Q}_i(\boldsymbol{\theta}_i^*)$, instead of the current point, $\mathcal{Q}_i(\boldsymbol{\theta}_i^*)$,

$$\boldsymbol{\theta}_i^{center} = \arg\min_{\boldsymbol{\theta}_{ik}} d(\mathcal{Q}_i(\boldsymbol{\theta}_{ik}), \bar{\mathcal{Q}}(\boldsymbol{\Theta}^*)) \tag{5}$$

where $\mathcal{Q}_i(\boldsymbol{\theta}_{ik})$ is the $k$th available samples on the manifold. Figure 1 pictorially shows how this procedure can help escape local minima.

## 4 Experiments

We have applied this approach to serial brain MRI scans with simulated and real atrophy (tissue shrinkage). In particular, longitudinally increasing atrophy was

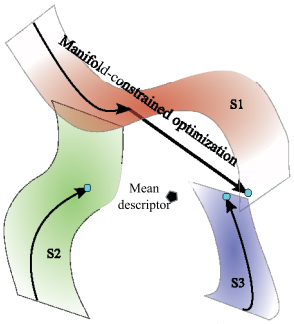


**Fig. 1.** Manifold-constrained optimization: the AEC of each individual resembles a manifold embedded in $R^N$, where $N$ is the dimensionality of the measurement space. An optimal member of each person's AEC is found by locally approximating the structure of this manifold with PCA, and iteratively traversing the manifold until a certain criterion of minimum variance is met. This procedure removes variations that are introduced by confounding variables during the calculation of a template transformation.

introduced to simulate the decrease of the gray matter associated with normal aging in a region on and around the superior temporal gyrus. Totally, 12 time points were simulated. For measuring real atrophy, we used the region of the hippocampus in serial scans of elderly individuals over a 4-year period. Due to the lack of ground truth in real datasets, we selected individuals with mild cognitive impairment (MCI), since for these individuals we expect to have longitudinal atrophy in the hippocampus. We then constructed AECs and then MAMs by varying registration parameters (smoothness as well as intermediate template) using the registration method of [3], as discussed in Section 2. We chose five intermediate templates with variable shapes in the regions of interest, and registered subjects in different resolutions, which is used to represent regularization. The optimization of Eq. (3) was used to estimate the optimal morphological representation (OMS) from each MAM. As expected, an intermediate template helps compute the OMSs with regularization close, but not same, to the most aggressiveness. For comparison, we also used the results obtained from a highly conforming registration, without intermediate templates or other parameter optimization. Mean values of the amount of gray matter brain tissue were finally computed in the regions where the atrophy was introduced, and are plotted against time points in Figure 2(a) (simulated atrophy) and (b) (real atrophy) to indicate the rate of atrophy for both traditional and proposed method.

Results indicate that our approach helps in eliminating confounding effects that are typical of fixed selection of templates and leads to a more stable temporal profile. On the other hand, the unoptimized measurements failed to detect temporal atrophy as shown in Figure 2(a) and (b). In addition, the unoptimized measurement is highly sensitive to the fixed selection of parameters, and, therefore, exhibits random fluctuations across time points. Although we don't have ground truth for real atrophy datasets, the two regions marked as "A" and "B" in Figure 3 show atrophy in the hippocampus and the medial temporal cortex, which are regions that we know are affected in MCI.

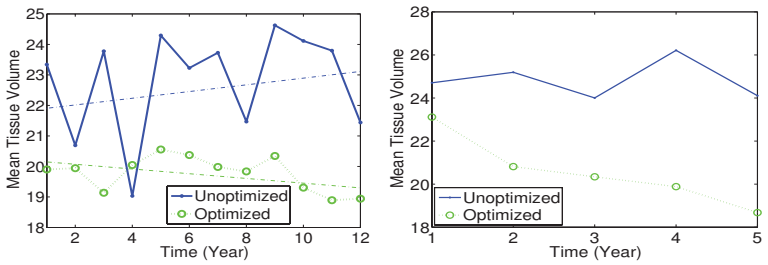


(a) (b)

**Fig. 2.** Comparison between most conforming CMD (traditional approach) and OMS in terms of mean GM TDM in the ROI in the presence of (a) simulated atrophy in Superior temporal gyrus, and (b) real atrophy.

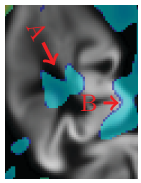


**Fig. 3.** The atrophy our method detected in the regions: A) hippocampus and; B) medial temporal cortex

## 5 Conclusions

In this paper, we proposed a framework for morphological analysis of medical images, and for group-wise registration, by building upon the work in [17]. The transformation from the template to an individual anatomy was combined with residual for a complete representation of anatomy, and each anatomy was represented through an equivalence class of descriptors, by varying transformation regularization and intermediate templates and constructing a morphological appearance manifold. We employed a minimum variance criterion and performed manifold-constrained optimization, i.e. traversed each individual's MAM, to find the points on all MAMs that brought the group of morphological descriptors closest to each other. We used local linear approximations of the manifold to follow the nonlinearity of a MAM. The proposed method can reduce the confounding variation in each MAM from noise, parameter and template selection, and preserve the true variations that relate to true underlying morphological change. This is confirmed in our experimental results, where our approach improves the performance of estimating longitudinal atrophy for simulated and real volumetric datasets.

## References

1. M. Miller, G. Christensen, Y. Amit, and U. Grenander, "Mathematical textbook of deformable neuroanatomies," *Proc. the National Acad. of Sciences* **90**(24), pp. 11944–11948, 1993.

2. M. Miller, A. Banerjee, G. Christensen, S. Joshi, and et al., "Statistical methods in computational anatomy," *Statis. Methods in Med. Research* **6**, pp. 267–299, 1997.
3. D. Shen and C. Davatzikos, "HAMMER: Hierarchical attribute matching mechanism for elastic registration," *IEEE Trans. Med. Imag.* **21**(11), pp. 1421–1439, 2002.
4. J. Ashburner and K. Friston, "Nonlinear spatial normalization using basis functions," *Hum. Brain Mapp.* **7**(4), pp. 254–266, 1999.
5. P. Thompson and A. Toga, "A surface-based technique for warping three-dimensional images of the brain," *IEEE Trans. Med. Imag.* **15**, pp. 402–417, 1996.
6. H. Johnson and G. Christensen, "Consistent landmark and intensity-based image registration," *IEEE Trans. Med. Imag.* **21**(5), pp. 450–461, 2002.
7. B. Karacali and C. Davatzikos, "Estimating topology preserving and smooth displacement fields," *IEEE Trans. Med. Imag.* **23**(7), 2004.
8. M. Miller, A. Trouvé, and L. Younes, "On the metrics and euler-lagrange equations of computational anatomy," *Annual Review of Biomed. Engin.* **4**, pp. 375–405, 2002.
9. C. Davatzikos, M. Vaillant, S. Resnick, J. Prince, S. Letovsky, and R. Bryan, "A computerized approach for morphological analysis of the corpus callosum," *J. Comp. Assis. Tomogr.* **20**(1), pp. 88–97, 1996.
10. J. Ashburner, C. Hutton, R. Frackowiak, I. Johnsrude, C. Price, and K. Friston, "Identifying global anatomical differences: deformation-based morphometry," *Hum. Brain Mapp.* **6**(6), pp. 348–357, 1998.
11. J. Ashburner and K. J. Friston, "Voxel-based morphometry – the methods," *NeuroImage* **11**(6), pp. 805–821, 2000.
12. C. Davatzikos, A. Genc, D. Xu, and S. Resnick, "Voxel-based morphometry using RAVENS maps: methods and validation using simulated longitudinal atrophy," *Neuroimage* **14**, pp. 1361–1369, 2001.
13. P. Thompson, J. Giedd, R. Woods, D. MacDonald, A. Evans, and A. Toga, "Growth patterns in the developing human brain detected using continuum-mechanical tensor mapping," *Nature* **404**(6774), pp. 190–193, 2000.
14. B. Davis, P. Lorenzen, and S. Joshi, "Large deformation minimum mean squared error template estimation for computational anatomy," in *ISBI'04*, pp. 173–176, 2004.
15. K. Bhatia, J. Hajnal, B. Puri, A. Edwards, and D. Rueckert, "Consistent groupwise non-rigid registration for atlas construction," in *ISBI'04*, pp. 908–911, 2004.
16. C. Twining, T. Cootes, S. Marsland, V. Petrovic, R. Schestowitz, and C. Taylor, "A unified information-theoretic approach to groupwise non-rigid registration and model building," in *IPMI'05*, pp. 1–14, 2005.
17. S. Baloch, R. Verma, and C. Davatzikos, "An anatomical equivalence class based joint transformation-residual descriptor for morphological analysis," *IPMI, 2007* **4584**, pp. 594–606, 2007.
18. M. B. Wakin, D. L. Donoho, H. Choi, and R. G. Baraniuk, "The multiscale structure of non-differentiable image manifolds," in *SPIE Wavelets XI, San Diego, Californi*, pp. 1–14, July, 2005.
19. J. Ham and D. D. Lee, "Separating pose and expression in face images: A manifold learning approach," *Neural Inform. Process. C Letters and Reviews* **11**(4-6), pp. 91–100, April-June 2007.
20. J. Tenenbaum, V. de Silva, and J. Langford, "A global geometric framework for nonlinear dimensionality reduction," *Science* **290**, pp. 2319–2323, 2000.
21. S. Roweis and L. Saul, "Nonlinear dimensionality reduction by locally linear embedding," *Science* **290**, pp. 2323–2326, 2000.